

11<sup>th</sup> ANKARA INTERNATIONAL AEROSPACE CONFERENCE  
8-10 September 2021 - METU, Ankara TURKEY

**AIAC-2021-065**

## **FLIGHT TIME CALCULATION OF A BLENDED-WING-BODY UAV THROUGH IMPROVED BLADE ELEMENT AND MOMENTUM THEORY**

Derya Kaya<sup>1</sup>, Ali Türker Kutay<sup>2</sup>, and Harun Özkanaktı<sup>3</sup>  
Middle East Technical University  
Ankara, Turkey

### **ABSTRACT**

*This study focuses on the conceptual design and flight-time calculation of a Vertical Take-Off and Landing-Blended Wing Body (VTOL-BWB) Unmanned Aerial Vehicle (UAV) through the Improved Blade Element and Momentum Theory (IBEMT) model developed in METU Aerospace Engineering Department. The IBEMT model is a physics-based method that estimates propeller forces and moments in all flight conditions using only the geometric information of the propeller by eliminating some assumptions in the classical BET. By applying the aerodynamic analysis tool XFLR5, the VTOL-BWB-UAV aerodynamic design methodology is established. Then, using the IBEMT model, the flight time of the aircraft is calculated.*

### **INTRODUCTION**

This paper presents the design of a VTOL-BWB UAV and its aerodynamic performance analyzed according to stability and control features. BWB is a type of aircraft configuration, which has an airfoil-shaped body contributing to overall lift during its flight. Its wing structure is smoothly blended into the body. The main advantage of the BWB design is its reduced wetted area to volume ratio compared to conventional aircraft which reduce the fuel consumption as well as structurally effective span loading. Because of the lack of tail and its unconventional shape, BWB's controllability and stability features become the most important part of the design. The VTOL-BWB UAV is designed to have five propellers and winglets instead of vertical fins. The aircraft is conceptually designed for low-speed flight conditions.

There are several studies in the literature, which examine the BWB UAV concept [Baig et al 2018, Panagiotou et al,2018, Lehmkuehler et al, 2021, Shim and Park, 2013]. NACA 25111 is proposed as the best possible option to be used in the center body because it has a high lift coefficient by Baig et al, 2018 [1]. To counter the negative moment by NACA 25111, the airfoil used in this section needs to have a higher positive moment coefficient. Therefore, MH 78 is chosen for the outer wing [Baig et al, 2018]. 3D Panel method results in XFLR5 are found to be very close to wind tunnel results [Baig et al, 2018]. Therefore, XFLR5 [6] is decided to be used in aerodynamic analyses of the aircraft.

---

<sup>1</sup>Graduate Research Assistant at METU Aerospace Engineering Department, Email: dekaya@metu.edu.tr

<sup>2</sup>Assist. Prof.Dr. at METU Aerospace Engineering Department, Email: kutay@metu.edu.tr

<sup>3</sup>Ph.D. Candidate at METU Aerospace Engineering Department, Email: ozkanak@ae.metu.edu.tr

## METHOD

Total span, take-off weight, and cruise speed are the requirements of the aircraft. Besides, it is aimed to have the VTOL ability as well as have more flight time compared to a drone. The mechanical simplicity is also the aim of this design. Therefore, none of the propellers used in the BWB UAV can tilt to get a mechanically simple aircraft. The conceptually designed BWB VTOL UAV is considered to hover and not to need a landing area like conventional aircrafts.

In consideration of their lift and moment characteristics, NACA 25111 and MH78 were selected for the center body and the wing respectively. The center of gravity is placed ahead of the aerodynamic center to provide longitudinal stability. Aerodynamic twist, dihedral, and sweep angle are included to increase stability and controllability. The final design was tested in XFLR5 for stability. BWB is very unstable in pitching moment because it doesn't have a tail section. Therefore, the location of the center of gravity is crucial for stability. Winglets are added at the wing tips for reducing the strength of wingtip vortices and improving lateral stability. A positive dihedral is given to improve the roll stability of an aircraft. Besides, sweep improves the yaw or lateral stability of an aircraft.

In XFLR5 analysis, Vortex Lattice Method (VLM) and 3D Panel Method can be used. The influence of the propellers, wing's thickness, and viscosity are ignored.

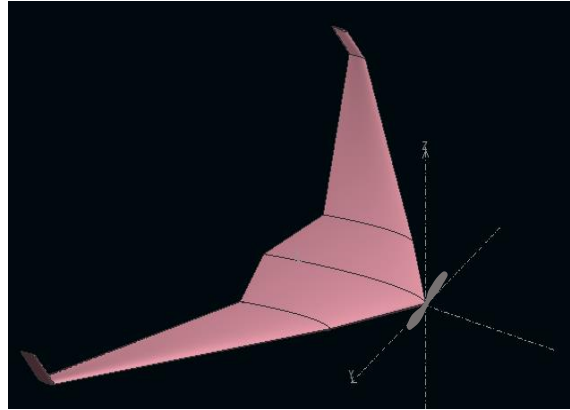


Figure 1: BWB UAV drawing in XFLR5.

The C.G.'s position is changed and stability is checked by XFLR5 stability analyses. Finally, it is placed 58% of the Mean Aerodynamic Chord (MAC).

Using the XFLR5 results, the variation of the lift coefficient with BWB's angle of attack,  $\alpha$ , is presented in Figure 2, and variation of the drag coefficient with BWB's angle of attack is given in Figure 3. Variation of the lift coefficient with drag coefficient is presented in Figure 4. Finally, the variation of the moment coefficient with BWB's angle of attack is shown in Figure 5:

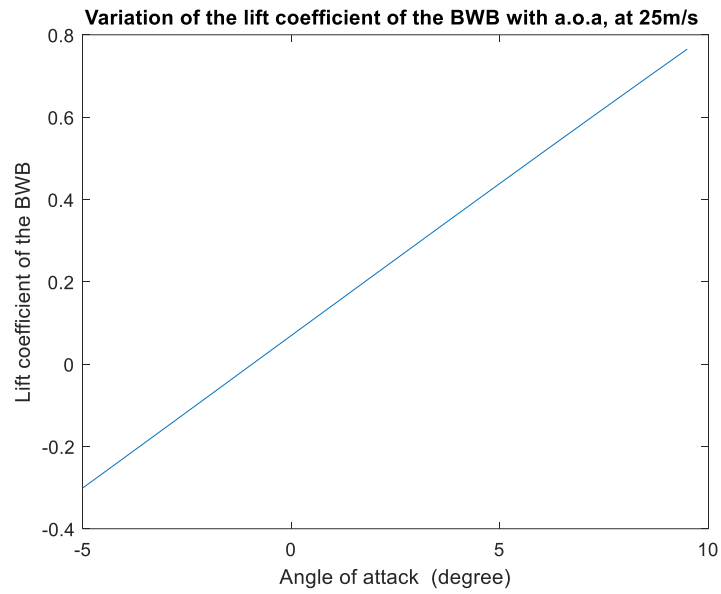


Figure 2: Variation of lift coefficient with angle of attack at 25  $m/s$  free-stream velocity.

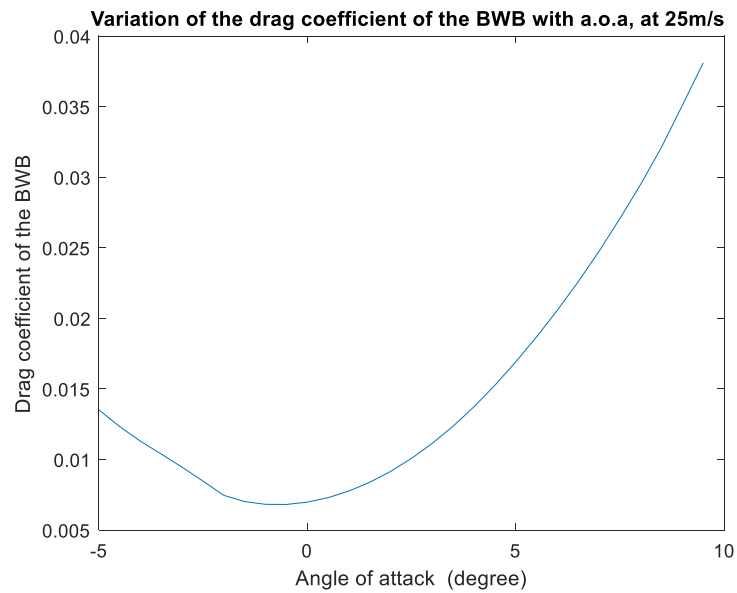


Figure 3: Variation of drag coefficient with angle of attack at 25  $m/s$  free-stream velocity.

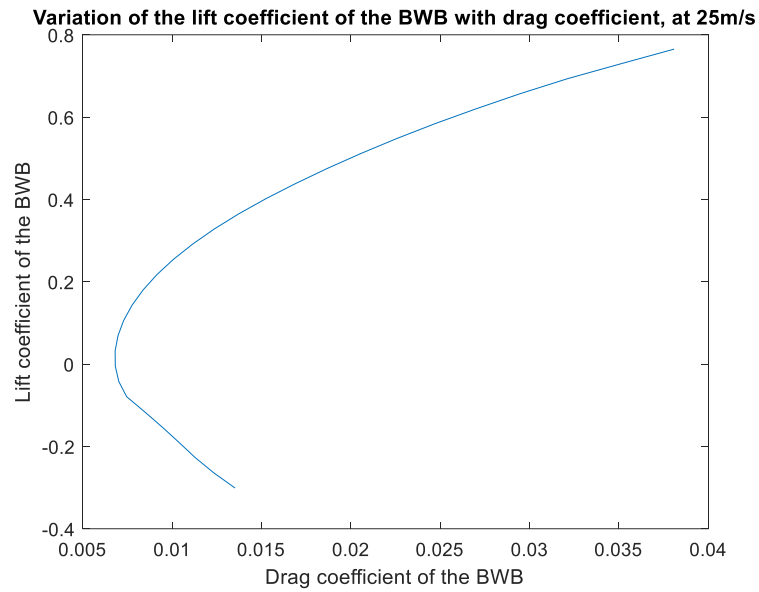


Figure 4: Variation of lift coefficient with drag coefficient at 25 *m/s* free-stream velocity.

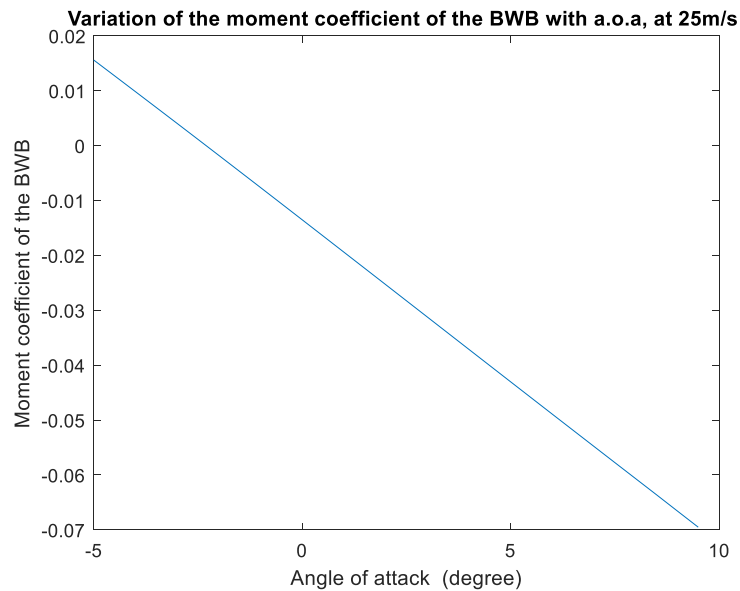


Figure 5: Variation of moment coefficient with A.o.A at 25 *m/s* free-stream velocity.

The BWB Aircraft parameters are given in Table 1:

Table 1: BWB Parameters used in conceptual design.

Total weight	6 kg
Wing span	3.2 m
Wing area	1.227 m <sup>2</sup>
Aspect ratio	8.346
Mean aerodynamic chord	0.511 m
Root chord	0.9 m
Dihedral angle	2° (body) 80° (winglets)
Location of C.G.	[0.303 0 0.006] m
Inertia	$\begin{bmatrix} 1.042 & 0 & 0 \\ 0 & 0.690 & 0 \\ -0.01566 & 0 & 1.730 \end{bmatrix} \text{ kgm}^2$
Wing loading	4.968 $\frac{\text{kg}}{\text{m}^2}$

The eigenvalues of the longitudinal and lateral modes of the aircraft are given in Table 2 and Table 3:

Table 2: Longitudinal modes.

Short period mode	$-11.9 \pm 8.227i$
Phugoid mode	$-0.00308 \pm 0.670i$

Table 3: Lateral modes.

Roll mode	-14.88
Dutch-roll mode	$-0.867 \pm 2.22i$
Spiral mode	0.00866

It is also possible to further improve this conceptual design by changing the location of C.G., sweep, twist, and dihedral angles, and then noting their effects on lift, drag, and moment variations with the angle of attack as well as longitudinal and lateral modes for stability. However, in this study, the BWB aircraft is designed for the implementation of the IBEMT model developed in [7]. Therefore, further analysis for conceptual design of a BWB UAV and adding vertical take-off and landing features to the aircraft is aimed as future work.

As seen in the Blended Wing Body (BWB) has four propellers inside the body to take off and land vertically, and to be controlled in hovering flight in all three axes like a quadrotor.

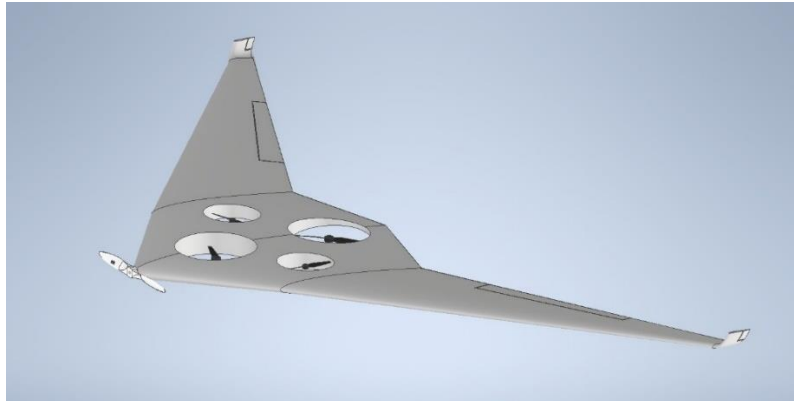


Figure 6: Conceptual design of VTOL Blended Wing Body UAV

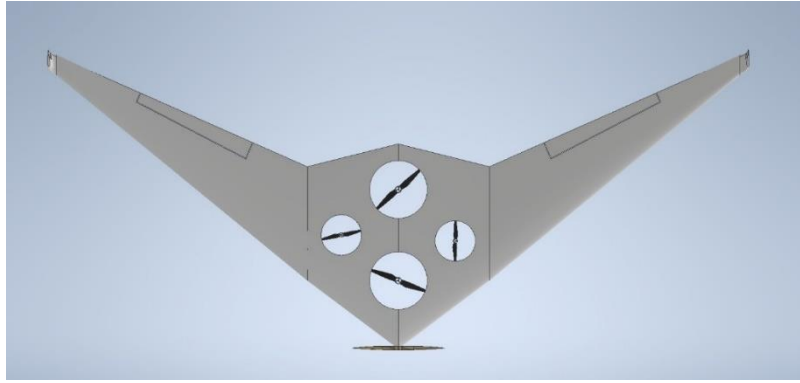


Figure 7: Top view of conceptual design of VTOL Blended Wing Body UAV

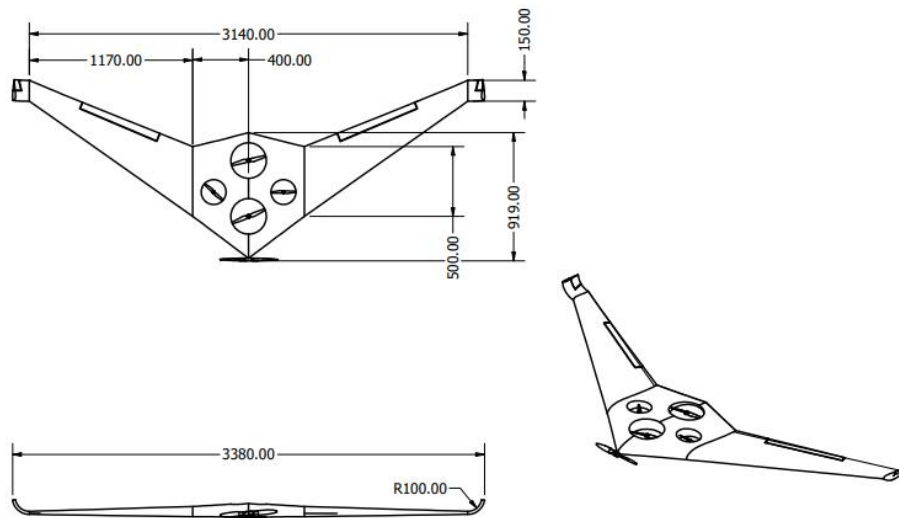


Figure 8: Technical drawings of the BWB (the unit is mm.)

As well, it has a propeller in front of the vehicle for supplying thrust force in forward flight. In forward flight, the surface of the propellers located in the body is aimed to be closed in order not to lose lift. The aircraft is controlled in forward flight by elevons located at the trailing edge of the wings and rudders located at the winglets. None of these propellers have the ability to tilt to make the aircraft mechanically simple.

Application of the BEMT model in a BWB UAV can be used as illustrated in Figure 9:

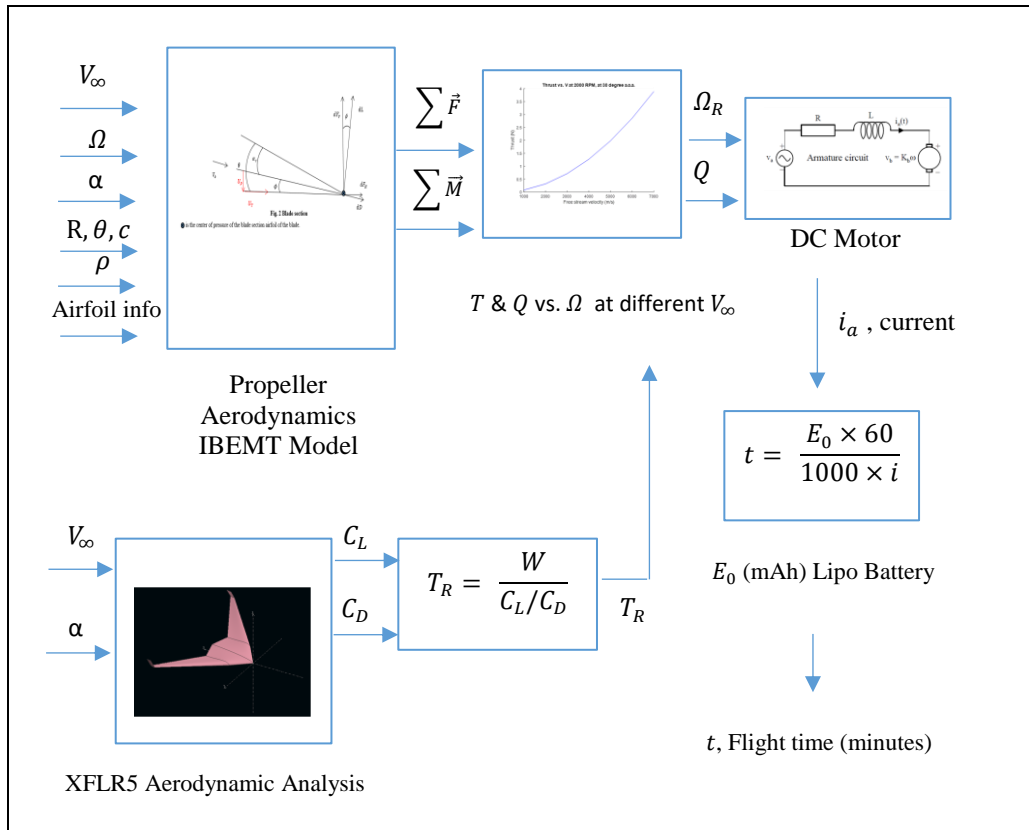


Figure 9: Flight time calculation using the IBEMT model [7]

The flight time of the UAV in steady-level flight is calculated as follows: In steady-level flight, lift generated by the aircraft equals to its weight:

For a given flight condition where the free-stream velocity is known, the required lift coefficient can be calculated in steady-level flight as follows:

$$C_L = \frac{W}{\frac{1}{2} \rho V_\infty^2 S_{ac}} \quad (2)$$

Since XFLR5 gives the  $C_L$  and  $C_D$  coefficients of the aircraft at different angles of attack, the corresponding  $\alpha$  values can be interpolated. Hence, the corresponding  $C_D$  coefficient is found at that  $\alpha$ . Then, the required thrust of the aircraft at a certain  $V_\infty$  is calculated as follows:

$$T_R = \frac{W}{C_L / C_D} \quad (3)$$

Table 4: Corresponding  $\alpha$ ,  $C_D$ , and  $T_R$  values at different free-stream velocities obtained from XFLR5 simulations.

$V_\infty$	15 m/s	20 m/s	25 m/s
$C_L$	0.3481	0.1958	0.1253
$\alpha$	5°	3°	2°
$C_D$	0.0183	0.013	0.00994
$T_R$	3.08 N	3.9 N	4.67 N

The thrust force of the aircraft is supplied by the propeller which is located as  $90^\circ$  A.o.A. in front of the aircraft. Since the IBEMT model estimates the propeller performance at any angles of attack,  $\Omega$  versus thrust values can be plotted at any  $V_\infty$ . Hence, the required propeller speed can be found by IBEMT model in less than 15 seconds.

The motor model is presented as follows (e.g. a DC motor):

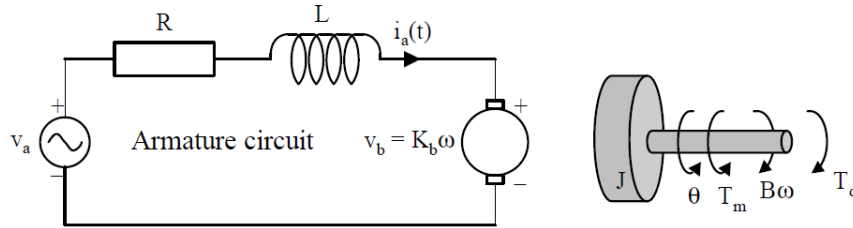


Figure 10: DC Motor [8]

By using Kirchoff's voltage law, the first equation is written as follows:

$$L_d \frac{di_a(t)}{dt} + R_d i_a(t) = v_a(t) - v_b \quad (4)$$

Using Euler's law, the second equation which will be used in modeling of a DC motor is written as follows:

$$J \frac{dw(t)}{dt} = T_m(t) - Bw(t) - T_d \quad (5)$$

$$\frac{dw(t)}{dt} = 0 \quad (6)$$

where,

$$T_m(t) = K_m i_a(t) \quad (7)$$

Then,

$$0 = K_m i_a - T_d - Bw \quad (8)$$

Hence, the relation between current and angular speed of the motor is written as follows:

$$i_a = \frac{T_d + Bw}{K_m} = \frac{T_d}{K_m} + aw \quad (9)$$

where  $a$  is a constant coefficient which can be found by least squares estimation using experimental data of the motor (i.e., the angular speed of the propeller, and corresponding torque and current values). In Equation (9),  $w$  also equals to the angular speed of the propeller,  $\Omega$  as well as angular speed of the motor and  $T_d$  is the torque produced by the propeller,  $Q$ . Then, Equation (2.68) is written as follows:

$$i_a = \frac{Q}{K_m} + a\Omega \quad (10)$$

In this study, T Motor MN5212 kV420, 15x5 in propeller data [9] is used. Then,  $a$  is found as  $2.88 \times 10^{-4}$ . Motor torque constant,  $K_m$ , is taken as 0.039.

Since the experimental data is captured by a physics-based method using Blade Element and Momentum Theory (the IBEMT model developed in [7]), the flight-time calculation is conducted using the developed model because it is fast compared to experimental and CFD studies.



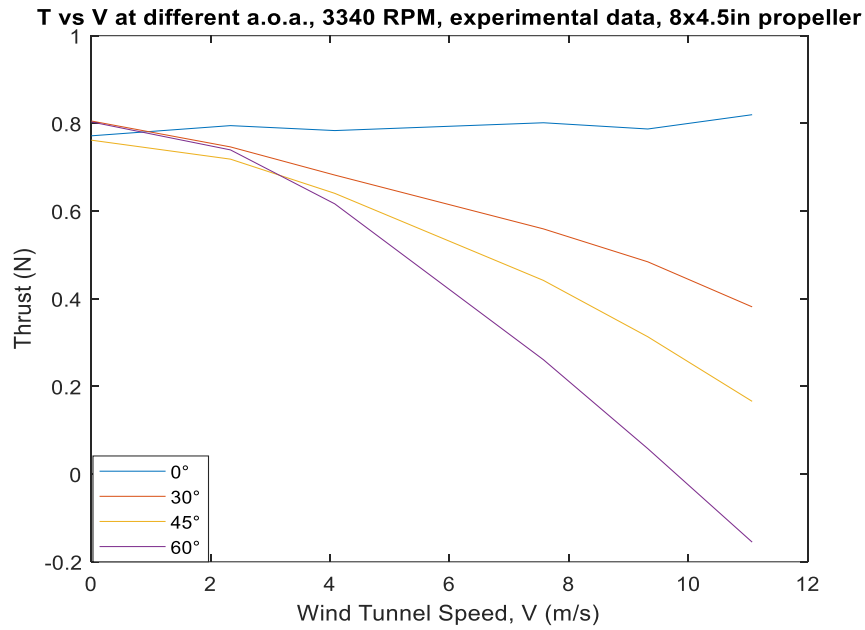


Figure 11: The experimental data [7].

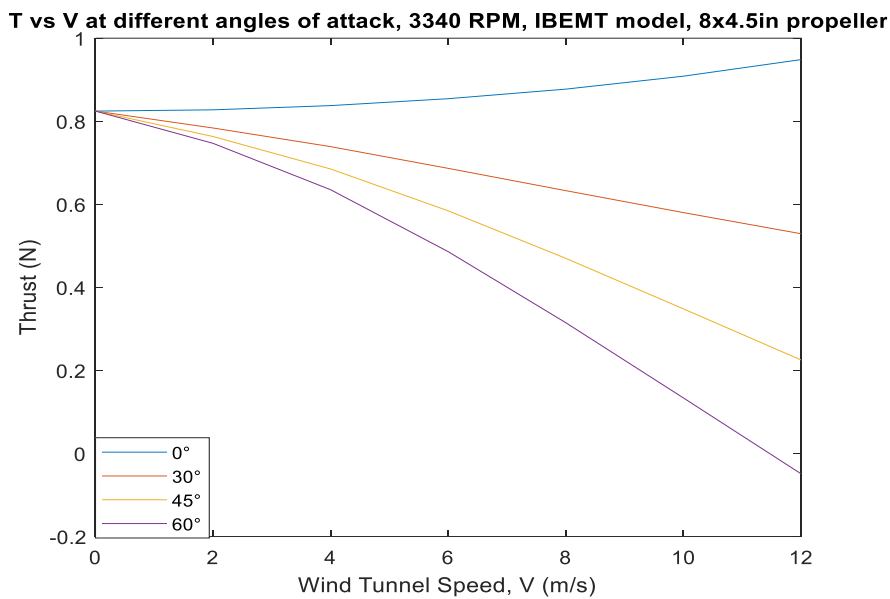


Figure 12: The IBEMT model [7].

## RESULTS

The application of the IBEMT model is presented on a BWB UAV using two propellers having two different  $\theta$  values. In the first case,  $\theta$  remains the same. In the second case, it is increased  $10^\circ$ . The steady-level flight is considered in  $15\text{ m/s}$ ,  $20\text{ m/s}$ , and  $25\text{ m/s}$ . Corresponding lift and drag coefficients in these flight speeds are found using XFLR5. Then, thrust required values are calculated at each flight condition. Angular velocity of the propeller that corresponds to thrust required value in  $15\text{ m/s}$  is found using Figure 13:

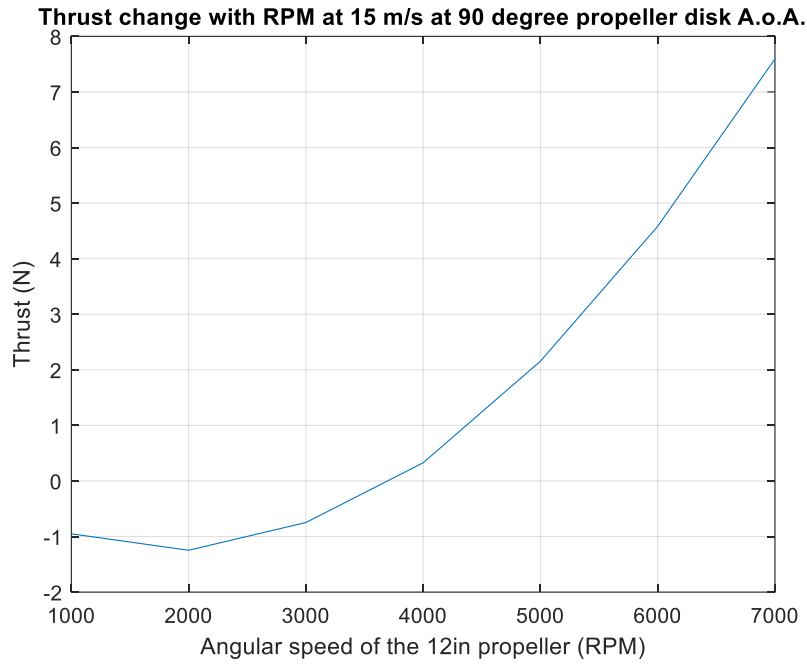


Figure 13: Thrust vs. RPM at 15 m/s,  $\theta + 0^\circ$ .

Rotor torque value that corresponds to  $\Omega_R$  is found through Figure 14:

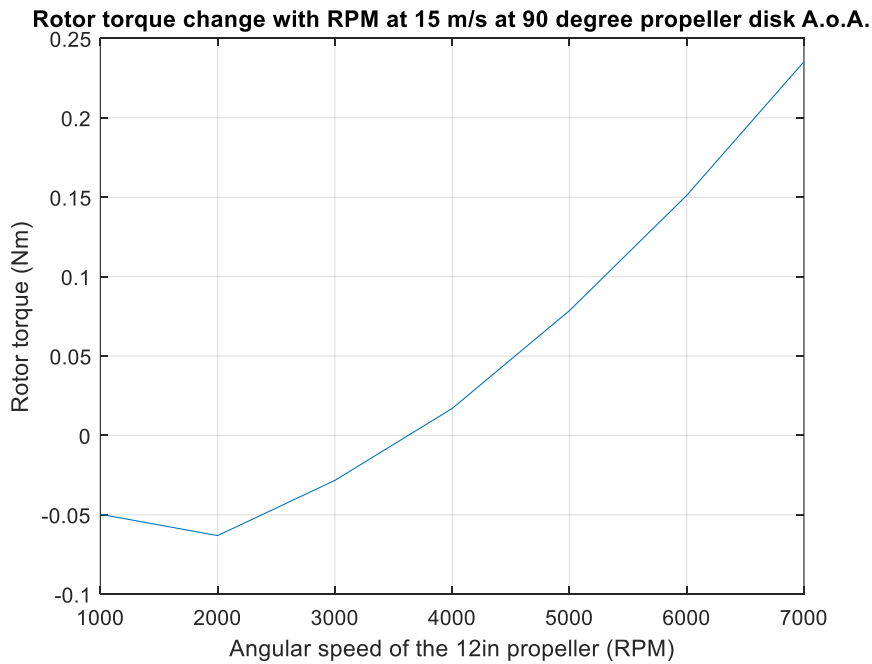


Figure 14: Rotor torque vs. RPM at 15 m/s,  $\theta + 0^\circ$ .

Same procedure is followed at  $V_\infty = 20 \text{ m/s}$  and  $V_\infty = 25 \text{ m/s}$ :

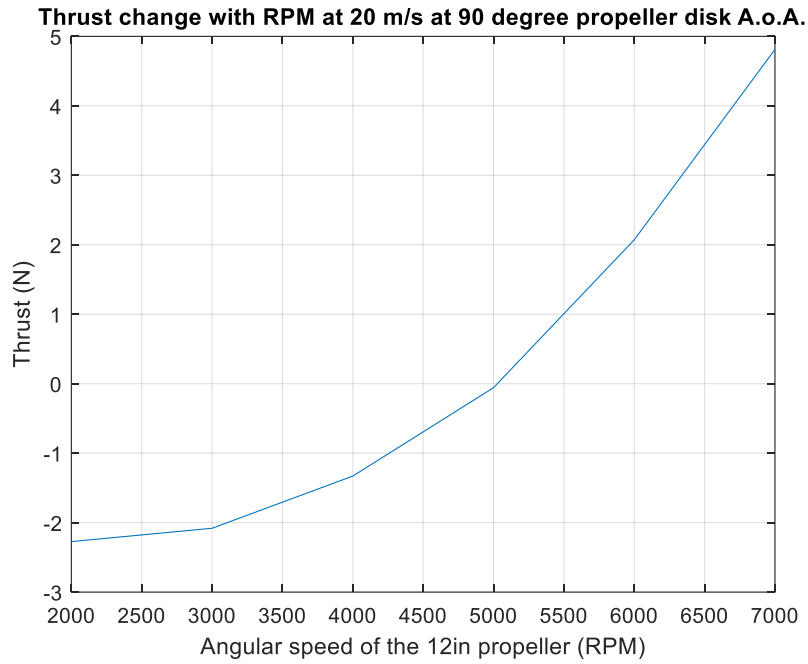


Figure 15: Thrust vs. RPM at 20 m/s,  $\theta + 0^\circ$ .

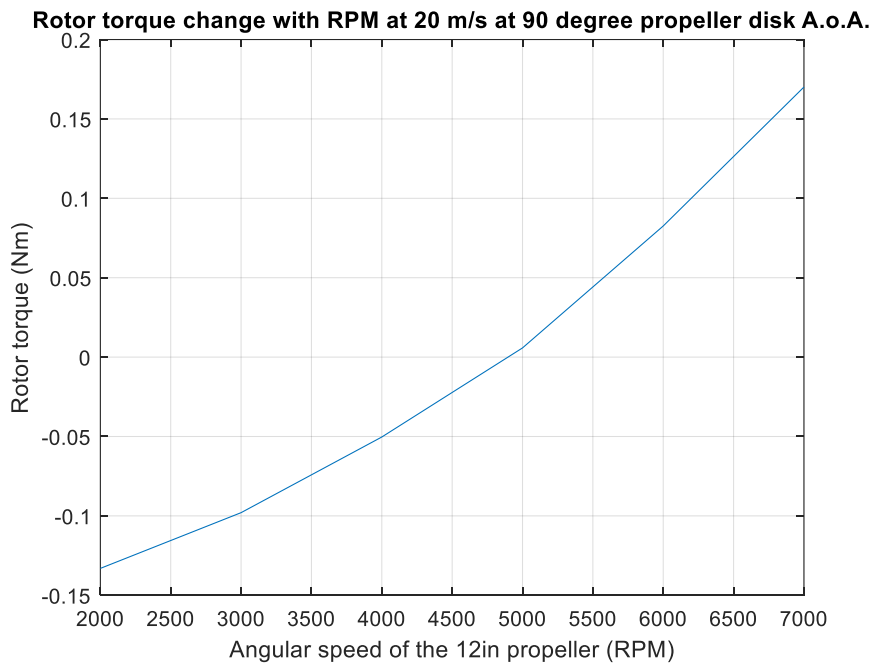


Figure 16: Rotor torque vs. RPM at 20 m/s,  $\theta + 0^\circ$ .

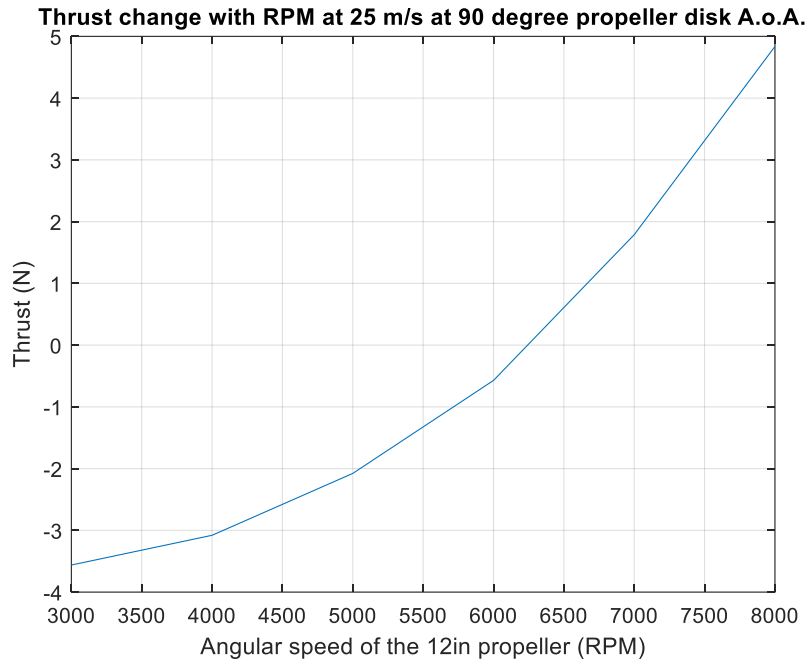


Figure 17: Thrust vs. RPM at 25 m/s,  $\theta + 0^\circ$ .

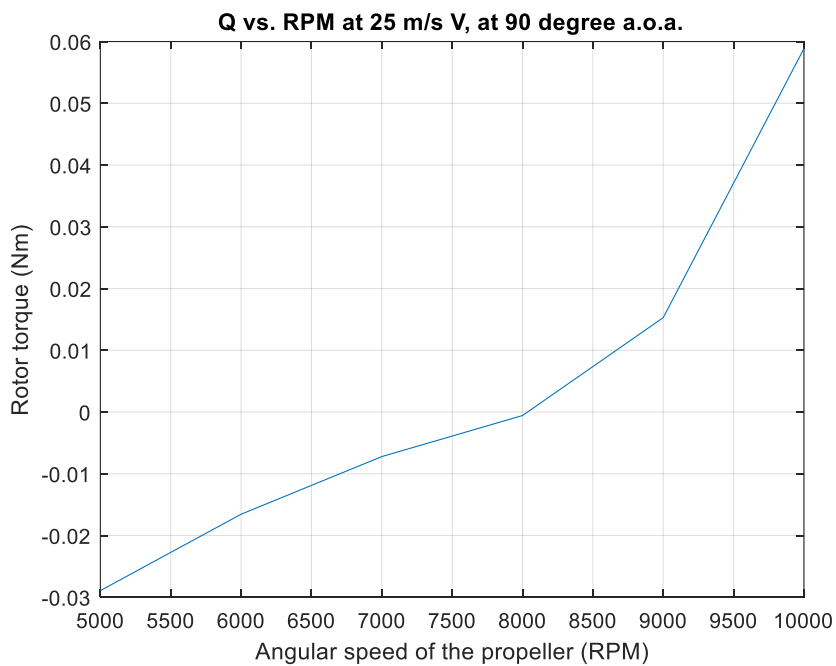


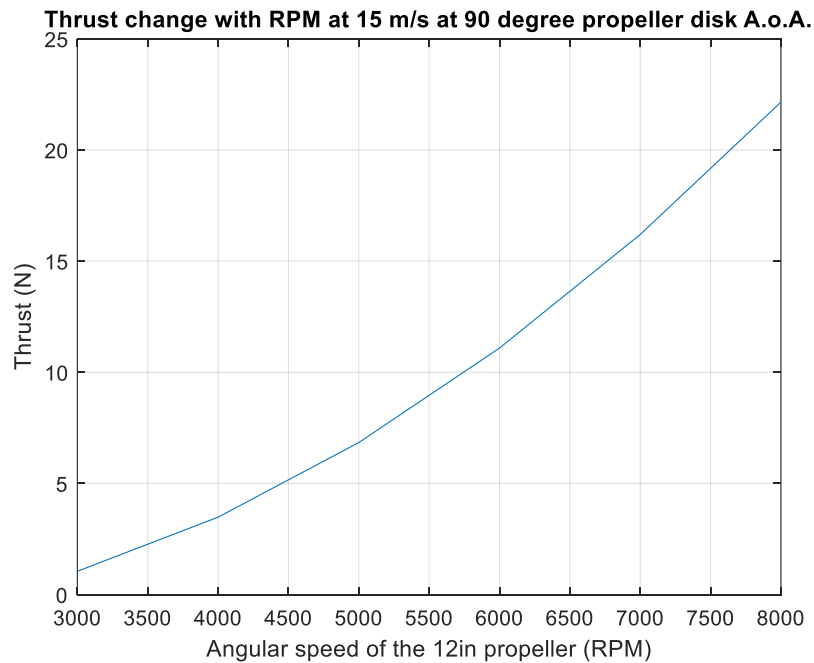
Figure 18: Rotor torque vs. RPM at 25 m/s,  $\theta + 0^\circ$ .

The flight time of the BWB UAV is shown in Table 5 using an 12in propeller with  $\theta$ :

Table 5: Results of Flight Time Calculation with  $\theta + 0^\circ$ 

$V_\infty$	15 m/s	20 m/s	25 m/s
$C_L$	0.3481	0.1958	0.1253
$\alpha$	5°	3°	2°
$C_D$	0.0183	0.013	0.00994
$T_R$	3.08 N	3.9N	4.67 N
$\Omega_R$ (RPM)	5350	6640	7940
$Q$ (Nm)	0.1	0.14	0.1750
$i_a$ (A)	3.95	6.86	10.26
$t$ (min)	75.93	43.70	29.23
Range (km)	68.33	52.44	43.84

Twist angle is increased  $10^\circ$  along the blade and the same procedure is conducted:

Figure 19: Thrust vs. RPM at 15 m/s,  $\theta + 10^\circ$ .

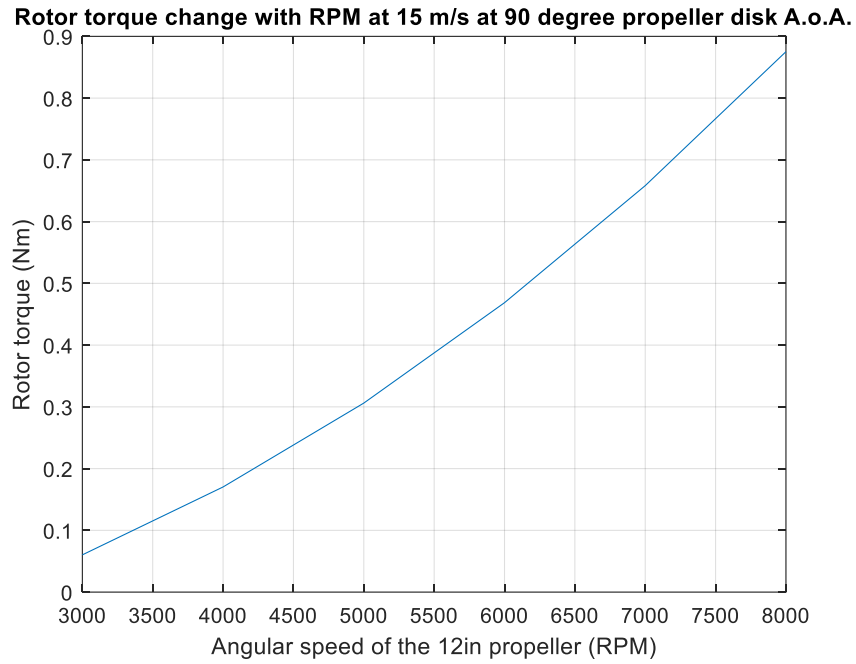


Figure 20: Rotor torque vs. RPM at 15 m/s,  $\theta + 10^\circ$ .

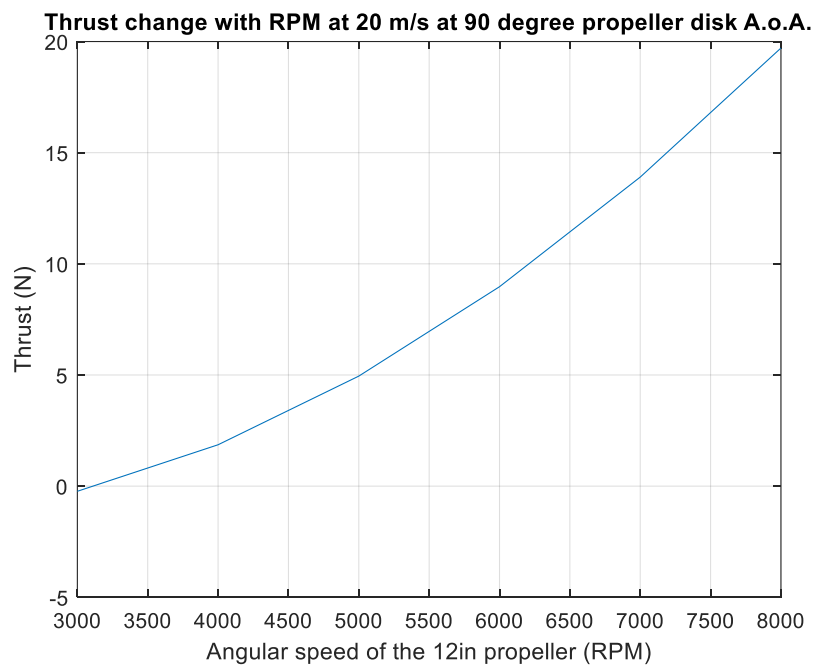


Figure 21: Thrust vs. RPM at 20 m/s,  $\theta + 10^\circ$ .

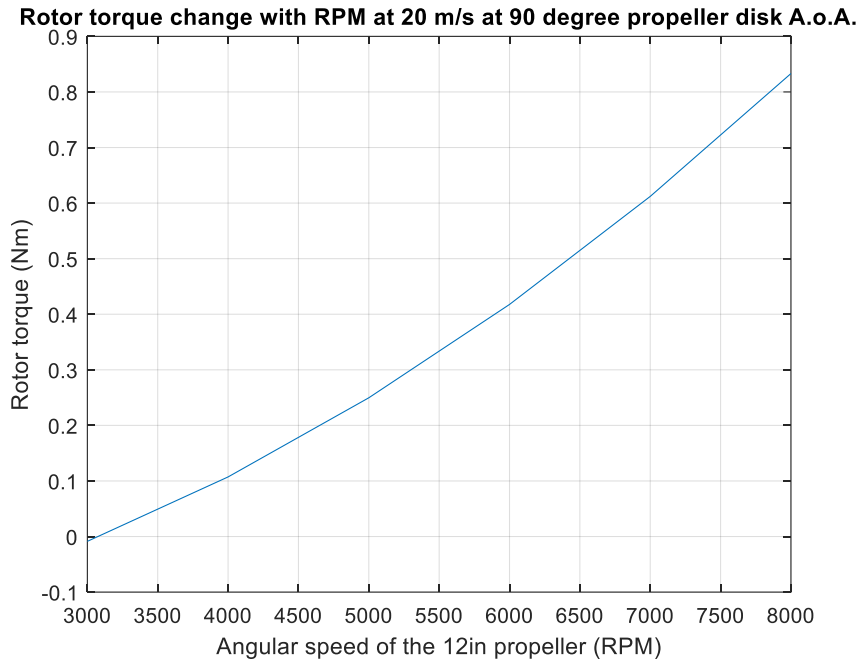


Figure 22: Rotor torque vs. RPM at 20 m/s,  $\theta + 10^\circ$ .

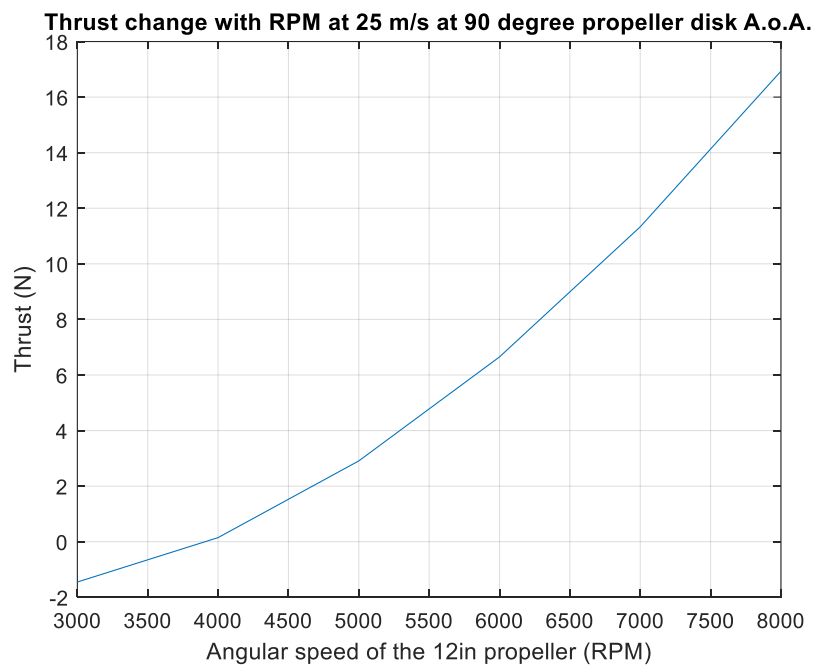


Figure 23: Thrust vs. RPM at 25 m/s,  $\theta + 10^\circ$ .

The flight time of the BWB UAV is shown in Table 6 using an 12in propeller with  $\theta + 10^\circ$ :

Table 6: Results of Flight Time Calculation with  $\theta + 10^\circ$ 

$V_\infty$	15 m/s	20 m/s	25 m/s
$C_L$	0.3481	0.1958	0.1253
$\alpha$	5°	3°	2°
$C_D$	0.0183	0.013	0.00994
$T_R$	3.08 N	3.9 N	4.67 N
$\Omega_R$ (RPM)	3850	4650	5440
$Q$ (Nm)	0.15	0.20	0.24
$i_a$ (A)	4.26	6.8677	9.6414
$t$ (min)	70.34	43.68	31.11
Range (km)	63.30	52.41	46.66

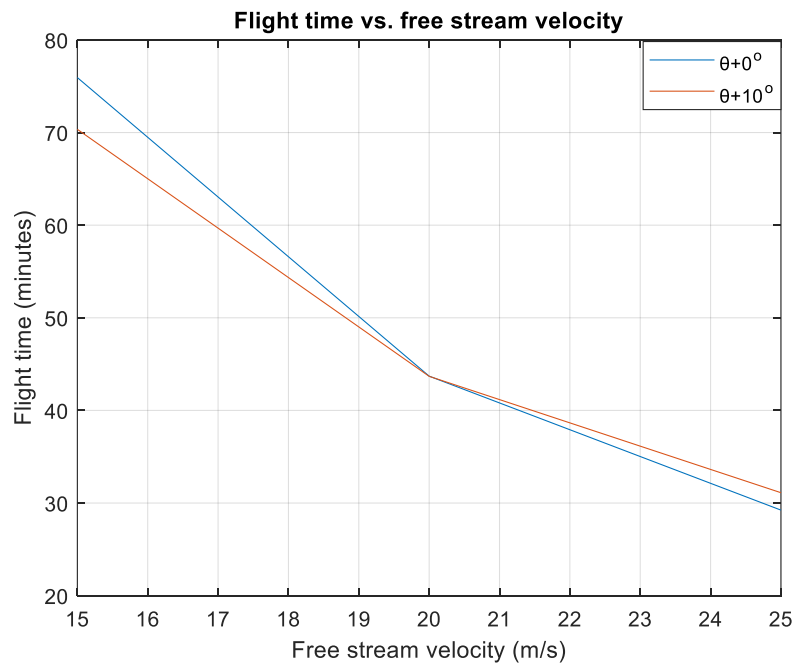


Figure 24: Total flight time comparison of the BWB VTOL UAV with different twist angles of the front propeller.

### CONCLUSION

In conclusion, a Blended Wing Body UAV is designed to demonstrate the application of the Improved Blade Element and Momentum Theory (IBEMT) model that can predict the propeller loads accurately not only in hovering flight unlike the classical Blade Element Theory but also in forward flight. As a result, the flight time of the BWB VTOL UAV is increased at 25 m/s when a propeller having a higher  $\theta$  (i.e.,  $\theta + 10^\circ$ ). Thus, the IBEMT model can be used for finding



the optimum propeller design for a UAV especially for a Vertical Take-Off and Landing Unmanned Aerial vehicle that has propeller configuration in both hovering and forward flight. Optimum propeller that gives the maximum flight time can be chosen or can be obtained using a variable-pitch mechanism according to the results obtained by the IBEMT model.

## References

- [1] Baig A. Z., Cheema T. A., Aslam Z., Khan Y. M., Sajid Dar H., Khaliq S. B., (2018), A New Methodology for Aerodynamic Design and Analysis of a Small Scale Blended Wing Body. J Aeronaut Aerospace Eng 2018, 7:1.
- [2] Panagiotou P., Fotiadis-Karras S., Yakinthos K., (2018), Conceptual design of a Blended Wing Body MALE UAV, Aerospace Science and Technology, Volume 73, Pages 32-47, ISSN 1270-9638, <https://doi.org/10.1016/j.ast.2017.11.032>.
- [3] Lehmkuehler K., Wong K.C., Verstraete D., (2012), Design and test of a UAV blended wing body configuration, in: Proceedings of the 28th Congress of the International Council of the Aeronautical Sciences, ICAS 2012, Brisbane, Australia.
- [4] Shim H.J., Park S.O., (2013), Low-speed wind-tunnel test results of a BWB-UCAV model, Proc. Eng. 67, 50–58, <https://doi.org/10.1016/j.proeng.2013.12.004>.
- [5] Wisnoe W., Nasir R.M., Kuntjoro W., Mamat A.M.I., (2009), Wind Tunnel experiments and CFD analysis of Blended Wing Body (BWB) Unmanned Aerial Vehicle (UAV) at Mach 0.1 and Mach 0.3, in: Proceedings of the Thirteenth International Conference on Aerospace Sciences & Aviation Technology, ASAT 2009, pp. 26–28.
- [6] XFLR5 analysis program. retrieved: <http://www.xflr5.tech/xflr5.htm>, 12.03.2021.
- [7] Kaya D., (2021), Estimation of Aerodynamic Loads of a Propeller through Improved Blade Element and Momentum Theory and Propeller Design Optimization, Ph.D. Thesis, Dept. of Aerospace Eng., Middle East Technical University, June 2021
- [8] Virgala I., Kelemen M., (2013), Experimental Friction Identification of a DC Motor. International Journal of Mechanics and Applications, 3(1): 26-30.
- [9] T Motor data, retrieved: <https://store.tmotor.com/goods.php?id=378>, 09.08.2021.